Comparison of measured and simulated icing in 28 test spans during a severe icing episode

Árni Jón Elíasson [1], Hálfdán Ágústsson [2], Guðmundur Hannesson[3], Egill Thorsteins[3]
[1] Landsnet, [2] Belgingur, [3] EFLA Consulting Engineers
arnije@landsnet.is, halfdana@gmail.com, gudmundur.m.hannesson@efla.is, egill.thorsteins@efla.is

***Abstract*: This paper presents an analysis of simulated in-cloud icing and a comparison of the results with detailed field measurements from 28 test spans at 19 test sites in North- and East-Iceland for a period of 99 days during the winter of 2013-2014. Ice accretion was extensive with the maximum ice load measured equal to 47 kg/m, the greatest total accumulation in one test span was 177 kg/m/winter and the total accumulation at the 28 test spans was 1076 kg/m/winter. The icing simulations are based on cylindrical accretion model using atmospheric data from a high resolution atmospheric model as an input.**

Model results are presented as time-series of icing at locations of test spans, as well as summaries of total accretion loads and intensities at the spans. Results are highly sensitive to the performance of the atmospheric model, while the timing of individual icing periods is nevertheless on average correctly captured. Small and medium size accretion events are generally better captured than more extreme events which are often underestimated due to too weak accretion intensity. In an attempt to remove the complicating and random effect of ice-shedding, the icing model is forced to shed ice in unison with the observations, with total simulated accretion compiled for each span during periods when accretion is actually observed.

Keywords: ***In-cloud icing, measurements, modelling, test spans***

INTRODUCTION

Long time series of systematic observations of atmospheric icing events are invaluable for mapping the icing climate and developing methods to parameterize icing. Accurate observations of extreme events are particularly important, especially within the framework of overhead power lines where appropriate design loads are critically dependent upon an accurate estimate of the maximum expected ice load for a given return period. Although, the observational sites are typically too few and far apart to describe adequately the spatial structure of the icing climate in complex orography, their data can be corroborated with parameterized icing based on simulated atmospheric data and numerical accretion models, as done for in-cloud icing in the USA, Japan and Iceland [1], [2], [3], [4].

In this light, the extreme icing winter of 2013-2014 presents an invaluable opportunity to test the current methods for parameterizing ice accretion and explore their strength and weaknesses. Special attention is given to the accretion process and the complicating influence of ice-shedding on the analysis is eliminated by forcing the accretion model to shed ice simultaneously with observed icing.

I. ICING MEASUREMENTS

Iceland has an extensive network of nearly 60 operational test spans at more than 40 locations, measuring ice accretion in real-time. Locations of test spans used in this study are shown in Figure 1.

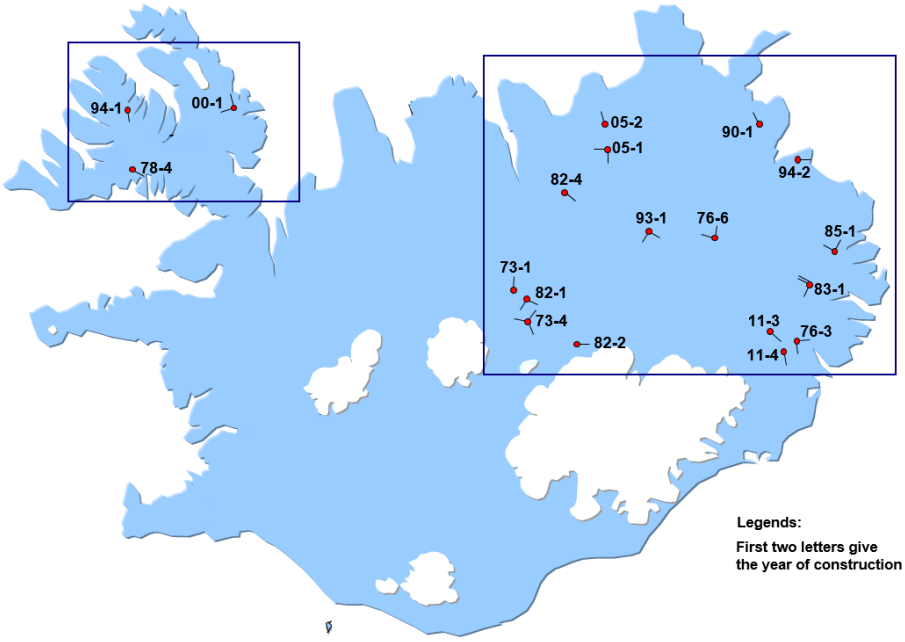

Figure 1: Locations of test span used in this paper, with black lines indicating the direction of each test span. Boundaries of the 1 km model domains are shown with black boxes.

In short, a test span consists of two poles with a conductor strung between them, in which the tension is measured in real-time with a load cell. A detailed description of the test setup is given in [5] and [6]. This setup may result in an overestimation of actual ice loading as the load cells measures the total load from both vertical (ice) and horizontal (wind) components. Other possible sources of uncertainty include calibration range of the load cells described in more detail in [7] or a change in base stringing during icing events.

Measurements from a sub-set of 28 test spans, in Northwest- and Northeast-Iceland (locations in Figure 1), are analyzed and compared with simulated icing. In short, the winter of 2013-2014 was characterized by extensive and more or less continuous ice accretion for 99 days from December to March in North- and East-Iceland, with two intense accretion periods from mid-December to mid-January, and again in February to early March. The maximum in-cloud ice load measured during the winter in a test span was 47 kg/m, the greatest total accumulation in a span during the period was 177 kg/m/winter and the total accumulation at the 28 test spans was 1076 kg/m/winter. The ice accretion was chiefly due to rime ice (in-cloud) and accreted wet-snow amounts were presumably minimal. The atmospheric and icing conditions are described in more detail in [7].

Four spans are located at an elevation of 500-600 m in the northwestern highlands. The orography is relatively simple with spans mostly located near the edges of a relatively flat plateau. Here the greatest ice accretion is expected at the northeastern margin of the plateau during northerly and northeasterly flow. Indeed, extreme icing was observed at test site 00-1 (Figure 2 and Figure 3) and caused a failure in early January, before the end of the accretion period. The remaining spans (23) are located in the northeastern part of Iceland. Those along the coast are generally located in complex orography while those in the highlands are in less complex orography. Here the main icing direction is from the northeast and east, with the highest loads expected at exposed mountain stations at the seaside. Three coastal sites; 90-1, 94-2 and 76-3, did indeed fail in early January due to the extreme ice loads.

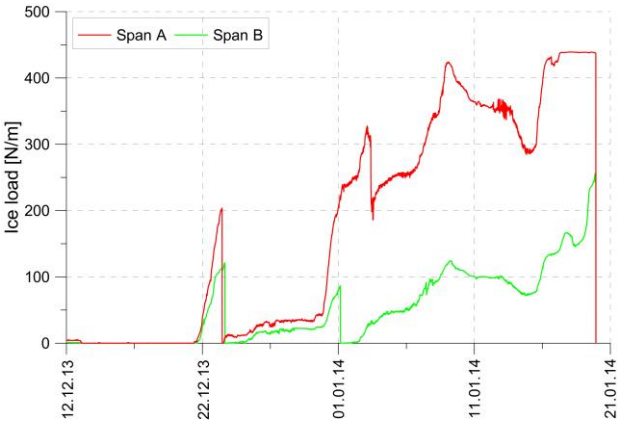

Figure 2: Ice load at test site 00-1. Both spans (00-1-A and 00-1-B) failed due to ice overload in January.


Figure 3: Ice on a guy wire in test span 00-1 after failure, the measured diameter was 47 cm.

II. Parameterization of Atmospheric Icing

Typically, in studies involving simulated icing, atmospheric models are used to simulate the state of the atmosphere at high resolution in complex terrain, making available all the necessary atmospheric parameters needed for estimating ice accumulation at any given location, based on numerical accretion models. For rime (in-cloud) icing these variables are the wind speed, air temperature as well as all the relevant atmospheric water species, namely cloud water and drizzle/rain.

A. Atmospheric data

Here, the atmospheric data is prepared with version 3.6.1 of the WRF model which is a state-of-the-art mesoscale atmospheric model [8] and has previously been used in a number of icing studies ([2], [5], [9]). The model was run with 55 layers in the vertical and a horizontal resolution of 9, 3 and 1 km, with the complex orography mostly resolved at a 1 km resolution. Results from the two 1~km model domains covering the two main regions of interest are used in the accretion modelling (cf. Figure 1 for domain locations).

The model was initialized and forced at its boundaries using the Interim atmospheric re-analysis data from the ECMWF ([10], resolution ~80 km). The most relevant parameterization schemes for studies of icing are the moisture physics scheme of Thompson ([11], [12]) which gives the necessary detail in the atmospheric water distribution needed to calculate both wet-snow and in-cloud accretion. The ETA planetary boundary layer scheme [13] is the second most relevant parameterization scheme employed and it should be noted that atmospheric stability and uplift, hence atmospheric water and precipitation distributions, are strongly linked to both the moisture physics scheme and the boundary layer scheme.

Since the actual orography is smoothed considerably at the resolution of the atmospheric model, the atmospheric data is interpolated linearly upwards at each grid point to the true elevation of the orography. As the aim is to seek an upper bound on maximum icing loads, no attempt is made to correct for overestimated terrain elevation.

The performance of the atmospheric model is analyzed based on a comparison with observations of weather from a dense network of automatic weather stations. Many of the stations are located in the lowlands and/or in coastal regions while some are located in the mountains with a few mountain top stations. As is frequently the case during icing episodes, observational data is lost, or it is unreliable, at many mountain stations. The model captures well the observations, with a mean temperature / wind speed bias of -0.1°C / 0.3 m/s and -0.6°C / 0.4 m/s in the northwestern and eastern domains, respectively. The mean bias is mostly well within ±1°C and ±1

m/s at individual stations but higher errors are generally found at stations where the orography is not well resolved by the model. There is significant temporal variability in the errors with the period after mid-February generally captured worse than earlier during the icing period. The overall accuracy of simulated data is considered adequate for input into the accretion model.

B. *The accretion model*

The simulated data described above is used as input to a time dependent numerical cylindrical ice accretion model, based on the model of Makkonen described in [14] and the methodology in [15]. The current study includes rime icing (in-cloud) as well as freezing drizzle and rain, but wet-snow is not considered. The icing rate is described by (1)

$$\frac{dM}{dt} = \alpha_1 \cdot \alpha_2 \cdot \alpha_3 \cdot w \cdot A \cdot V \qquad (1)$$

where M(t) is the accreted ice mass (kg), V is particle velocity (m/s), A is the cross-sectional area (m^2) of the cylinder as seen by an impinging particle, and w is the liquid water content (kg/m^3) of the particle and is chiefly due to cloud water but also due to drizzle and rain. V is here taken as the wind speed, with the size dependent fall speed of rain and drizzle particles taken into account. The three α-coefficients can generally take values between 0 and 1, and are given by: α_1 which is the collision efficiency and is calculated based on [16] and a median volume diameter (MVD) of the impinging water particles and a fixed droplet number N_d = 50 droplets/cm^3. α_2 is the sticking efficiency and is taken as 1 as it is generally assumed that all impinging particles will stick to a wet as well as a dry accretion surface. α_3 is the accretion efficiency and is calculated based on estimates of the heat balance at the accretion surface (see in [15] and references therein), and may deviate significantly from 1 during wet growth when the latent heat released at the accretion surface is not removed efficiently enough (generally occurs at high accretion intensity, during weak winds and when temperatures are only slightly negative). The density of the accreted cloud water (rime ice) is parameterized based on equation (4.1) in [15] while for freezing drizzle/rain the density is taken as 917 kg/m^3 (clear ice).

Icing calculations are done for a horizontal cylinder representing the conductor at 28 test spans and at 19 locations, taking into account individual span direction and conductor diameter. Furthermore, at each span an account is kept of simulated ice accretion concurrent with observed accretion (type A), as well as of accretion simulated when none is observed (type B).

C. *Ice shedding*

Ice shedding must be taken into account in modeling of in-cloud icing, especially in areas characterized by extreme and frequent icing conditions and where the temperature is on average near or below freezing. Main factors for ice shedding are: (i) melting, (ii) sublimation and (iii) mechanical ice break. Some attempts have been made to model ice shedding but no widely accepted model exists that has been validated with sufficient field data. Some models ignore (iii) but they can severely underestimate the intensity of ice loss processes.

Ice shedding is partly a stochastic process as can be seen in Figure 4, which shows measurements from three spans at the test site 83-1. Two spans (A and C) are parallel and have different conductor diameters while the third span (B) is oriented perpendicular to them and has the same conductor diameter as span A. A visual comparison shows that the ice shedding is occurring at different times in the spans.

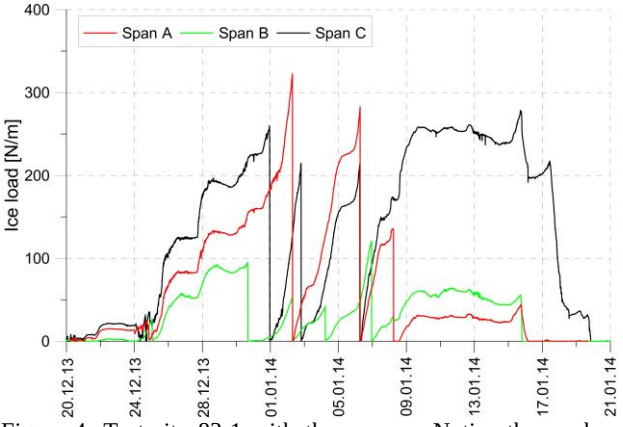

Figure 4: Test site 83-1 with three spans. Notice the random nature of ice-shedding.

The effect of ice-shedding is eliminated from the analysis of the simulated accretion process by forcing the accretion model to shed ice in unison with observed ice shedding at individual spans. During periods when there is no observed ice accretion, and hence no observed shedding, ice shedding within one hour (dm_{shed}) is simply parameterized as in (2), which has previously given reasonable results in studies of in-cloud icing.

$$dm_{shed} = max \begin{cases} k_{break} \cdot M_{ice} \\ k_{sublim} \cdot \pi \cdot D \end{cases} \qquad (2)$$

with the shedding factor associated with ice fall given by

$$k_{break} = \begin{cases} \frac{1}{3}(1 + 0.075 \cdot V) \;\; if \; T > 0°C \\ \frac{1}{3} \; if \; T + 0.05 \cdot V > 0 \; and \; T \leq 0 \\ 0 \; otherwise \end{cases} \qquad (3)$$

Here M_{ice} is the accreted mass of ice (kg), D_{ice} is the icing diameter (m), T is the air temperature (C) and k_{sublim} is an estimated shedding factor associated with sublimation (0.00125 gr/m^2/hour).

III. Results of Accretion Calculations

Ice accretion was simulated at 28 test spans, with 4 spans located in Northwest Iceland and 24 located in Northeast-Iceland. Figure 5 to 12 show examples of observations and ice modelling at eight of the test spans:

- The figures illustrate clearly how the model is forced to shed the accreted ice in unison with the observations.
- The timing of observed accretion is usually well captured.
- While some accretion periods are well captured there are cases where the observed accretion intensity and the ice load are either overestimated or underestimated.
- Large biases in overall accretion are found at some spans, including 83-1-A where smaller accretion events are very well predicted but the accretion intensity is too weak in the three largest events

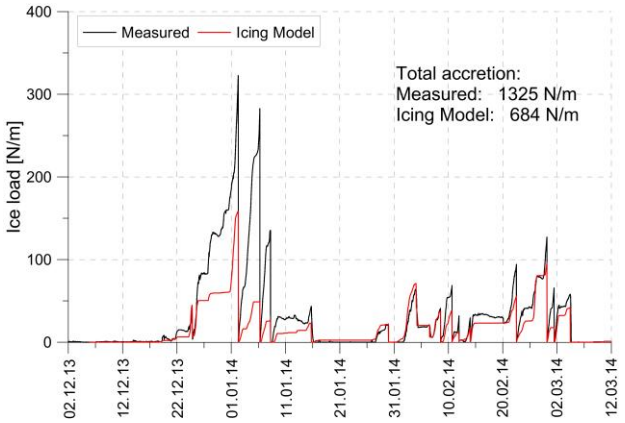

Figure 5: Measured and modelled icing in test span 83-1-A.

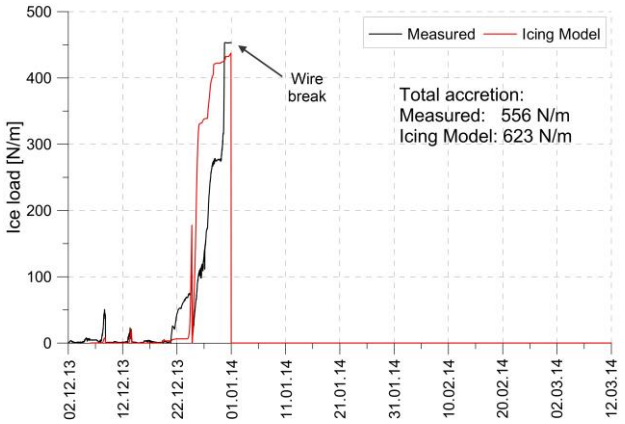

Figure 6: Measured and modelled icing in test span 94-2-A.

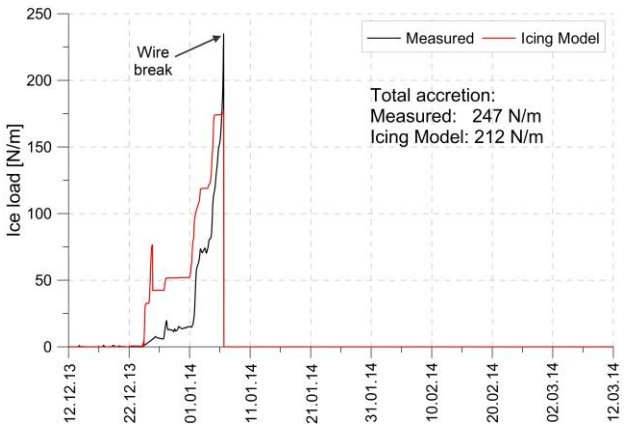

Figure 7: Measured and modelled icing in test span 76-3-B.

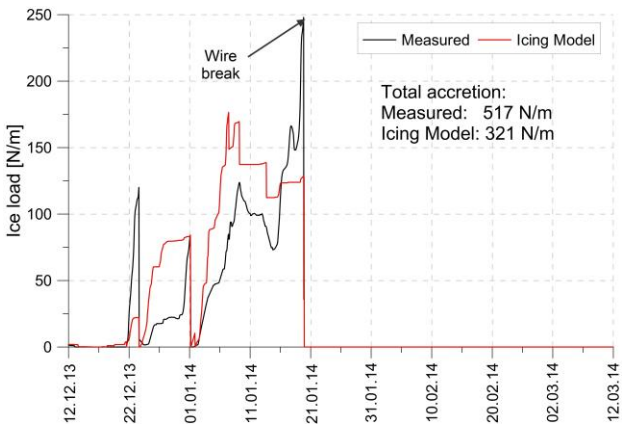

Figure 8: Measured and modelled icing in test span 00-1-B.

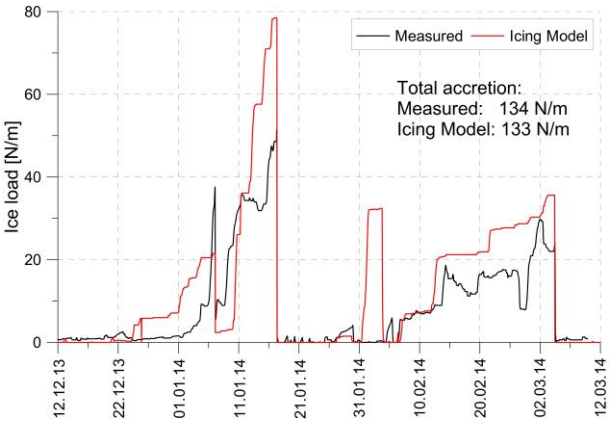

Figure 9: Measured and modelled icing in test span 11-4-A.

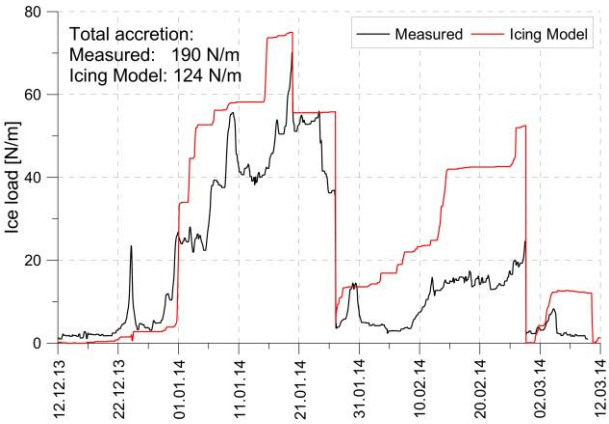

Figure 10: Measured and modelled icing in test span 73-4-A.

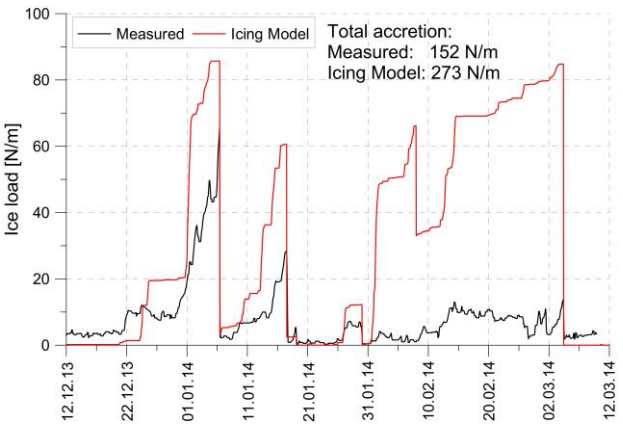

Figure 11: Measured and modelled icing in test span 11-3-A.

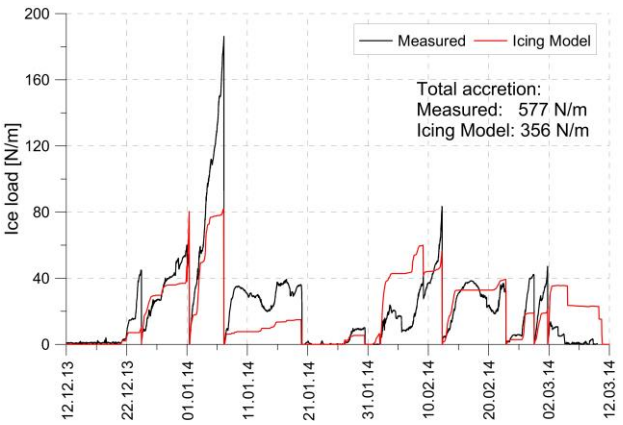

Figure 12: Measured and modelled icing in test span 82-4-A.

Figure 13 shows the overall observed icing and accretion simulated during periods when icing is observed (type A), i.e. ignoring accretion in the icing model when no ice is on the test span. The total accumulated observed and simulated loads at individual test spans generally compare favorably at locations where icing amounts are small or moderate. There is, however, a tendency towards underestimating the observed icing, especially at large icing amounts. The most significant outliers include test site 83-1 (3 spans) where only about half of the total accumulation is simulated and test site 85-1 where the accretion is significantly overestimated.

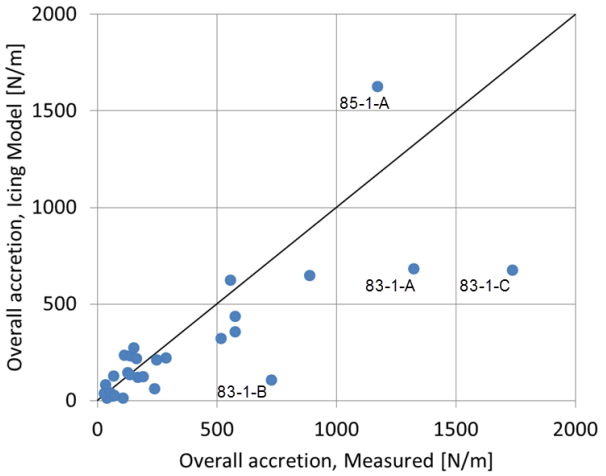

Figure 13: Observed and simulated total accumulation during the winter.

A comparison of the maximum icing observed and modelled in the period reveals that the maximum observed load is on average reasonably captured (Figure 14).

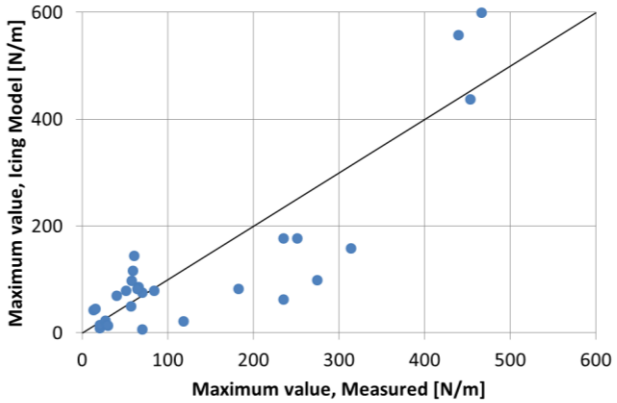

Figure 14: Comparison of calculated and measured maximum ice load over the winter 2013-2014.

Figure 15 presents a different method of assessing the overall performance than is presented in Figure 13. The time series of accumulated accretion are summarized over all the spans and simulated accretion is shown for periods when accretion is observed (type A) and also including periods when none is observed (type A+B), i.e. A is accretion at same time as ice is observed and B is when no ice is observed. Ice accretion starts in December and the first intense accretion period are in late December 2013. There is an apparent decrease in accretion intensity in early January 2015, after which the intensity is approximately half of what it was before. This decrease is associated with a mechanical failure of 5 spans and hence the subsequent analysis includes a reduced number of operational test spans. The greatest accretion intensities and largest ice loads were measured at some of the test spans that failed.

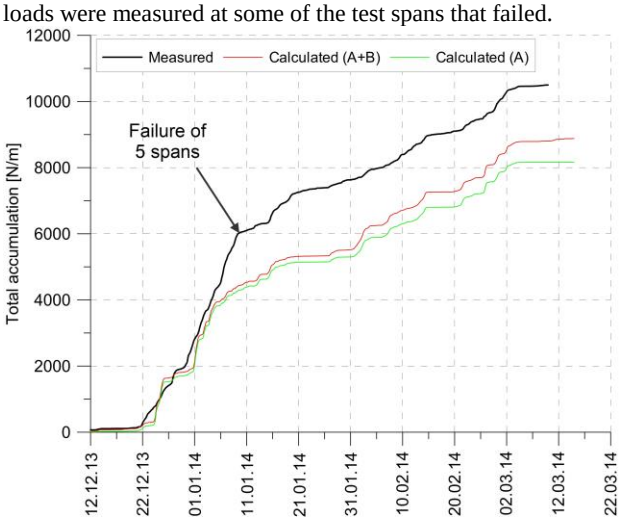

Figure 15: Total ice accretion in all spans, during the winter 2013-2014.

Figure 15 reveals that the total amount of modelled icing is following the measured icing reasonably well. The exception is the period 05-09 January 2014 when it is underestimating the accretion. The underestimation is largely related to the three test spans at test site 83-1, Figure 5 shows test span 83-1-A.

A sensitivity test was made, where icing conditions were modified to enhance the ice accretion. The atmospheric water content and wind speed were increased by 10% and the observed temperature was lowered by 1°C and used instead of simulated temperature. This analysis (not shown) reveals that the total amount of ice accretion increases and exceeds the observed accretion in Figure 15. Accretion has increased at test site 83-1 in the period 05-09 January 2014 although it is still lower than measured.

In the context of analyzing sensitivity to small variability in the atmospheric parameters then it should be noted that the icing model was analyzed assuming a fixed droplet number N_d = 50 droplets/cm^3. This implies rather large droplets sizes and consequently a relatively high accretion rate due to an enhanced collision efficiency factor (α_1), compared to larger values of Nd.

IV. Discussion and Concluding Remarks

Overall the results of the study are promising and show that coupled atmospheric and accretion models can be used to quantify and analyze atmospheric icing in complex terrain. The onset of ice accretion is generally correctly captured and the performance of the accretion model is on average good, both in a regional context as well as locally. The size of the observed ice load at individual spans varies greatly and includes eight test spans with loading in range of 20 to 46 kg/m. No systematic deviations were found at different magnitude of modelled accretion. Before discussing the most relevant deviations in more detail then it should be noted that there is, as previously mentioned, some uncertainty in the measured ice load which may partly explain the difference between measured and modelled ice load. It is however unlikely that the largest errors, e.g. at test site 83-1 (Figure 5) can be explained by complications in the measurement process.

The largest part of the negative bias seen in the accretion series presented in Figure 15 is obviously associated with the outliers in Figure 13, where the large observed accretion amounts are in some cases not as well captured. A large part of the bias is related to the three test spans at site 83-1 in the period 05-09 January 2014. Many of the smaller icing accretion

periods are well modelled in 83-1 (see Figure 5) but the most intense accretion is underestimated. The local topography at test site 83-1 is not too complex and the state of the atmosphere should therefore be reasonably well captured. Here, as well as at most other locations, the air temperature is on average reasonably captured and the icing model performance does not change significantly when observed temperatures are used instead of simulated temperatures. Comparison with lowland locations where instrumental icing is not a problem reveal that wind speeds are generally well reproduced but this is not necessarily true for nearby mountain stations. Significant and realistic quantities of atmospheric water are simulated at test site 83-1 but unfortunately no observational data is available for verification purposes. A sensitivity test, where icing conditions were made more favorable, reveals that realistic errors in the atmospheric conditions can explain a part of the poor performance in the period 05-09 January 2014. With respect to the accretion sensitivity it should be noted that the selected value of droplet size (N_d=50 droplets/cm^3) leads to a rather high accretion rate.

Test site 85-1 shows the largest overestimation of modelled ice accretion. It is located in very complex terrain which cannot be reproduced in the 1 km numerical domain. The temporal structure of the ice accretion at the site furthermore differs significantly from most of the other sites in the region. Thus it is not unexpected that test site 85-1 performs badly.

In general, errors in simulated atmospheric data can mainly be traced back to three factors:

- Inaccuracies in the input data from the courser model, i.e. in this case the boundary and initial data from the ECMWF. However, this does not seem to be of importance here, except possibly during the period 5-9 January 2015.
- Errors in the parameterizations of physical processes, e.g. boundary layer effects and precipitation processes. This may be relevant but is hard to verify due to the lack of observational data, e.g. of atmospheric water content.
- Local and small scale effects not resolved at the resolution of the atmospheric model. This is presumably the main source of error at many locations in complex terrain and may also be valid in simpler terrain if very small scale features disrupt the local flow.

Modelling of ice-shedding is an important factor when assessing extreme ice load in areas prone to frequent in-cloud icing. Here, the effect of the ice-shedding can be eliminated from the analysis by forcing the accretion model to shed ice in unison with observed ice shedding at individual spans. Example of the importance of the ice-shedding can been seen in Figure 5, where the largest ice load would be much higher, in early January, if there were not three cases of ice-shedding in the period.

The analysis presented in this study is made possible by the detailed observations available from a large number of test spans. The overall performance of icing model is good at the observational sites. This indicates that the accretion model is in general also reliable at other locations and its results can be used to assess ice loads in complex terrain where observational data is generally sparse or missing.

REFERENCES

[1] G. Thompson, Nygaardm B. E., L. Makkonen, and S. Dierer, "Using the Weather Reserach and Forecasting (WRF) Model to Predict Ground/Structural Icing," in *13th IWAIS*, Andermatt, 2009.

[2] Á. J. Elíasson, H. Ágústsson E. Þorsteins, and Ó. Rögnvaldsson, "Comparison between simulations and measurements of in-cloud icing in test spans," in *Proc. 14th Int. workshop on atmospheric Icing on structures*, China, 2011, p. 7.

[3] B. E. K. Nygaard, Kristjánsson. J. E., and L. Makkonen, "Prediction of In-Cloud Icing Conditions at Ground Level Using the WRF Model," *J. Appl. Meteor. Climatol.*, vol. 50, pp. 2445-2459, 2011.

[4] E. A. Podolskiy, B. E. K. Nygaard, K. Nishimura, L. Makkonen, and E. P. Lozowski, "Study of unusual atmospheric icing at Mount Zao, Japan, using the Weather Research and Forecasting model," *J. Geophys. Res.*, vol. 117, p. 12106, 2012.

[5] H. Ágústsson, Á. J. Elíasson, G. M. Hannesson, and E. Thorsteins, "Modeling wet-snow accretion -- Comparison of cylindrical models to field measurements," in *Proc. 15th International Workshop on*, Canada, 2013, p. 9.

[6] Á. J. Elíasson and E. Thorsteins, "Ice loadmeasurements in test spans for 30 years," in *Proc. 12th Int. Workshop on Atmospheric Icing of Structures (IWAIS)*, Yokohama, 2007, p. 6.

[7] Á. J. Elíasson and E. Sveinbjörnsson, "A severe In-cloud Icing Episode Mid-winter 2013-2014 in Northern and Northeastern Iceland ," in *Proc. 16th International Workshop on Atmospheric Icing of Structures*, Uppsala, 2015.

[8] W. C.: Klemp, J.B. Skamarock et al., *A description of the advanced research WRF version 3*.: NCAR: Boulder, 2008.

[9] B. E. K. Nygaard, H. Ágústsson, and K, Somfalvi-Tóth, "Modeling wet snow accretion on power lines: Improvements to previous methods using 50 years of observations," *Journal of Applied Meteorology and Climatology*, vol. 52, no. 10, pp. 2189-2203, 2013.

[10] D. P. Dee, S. M. Simmons, A. J. Berrisford, P. Poli, and co-authors, "The ERA-Interim reanalysis: configuration and performance of the data assimilation system," *Q. J. Roy. Meteorol. Soc.*, vol. 137, no. 656, pp. 553-597, 2011.

[11] G. Thompson, R. Rasmussen, and K. Manning, "Explicit forecasts of winter precipitation using an improved bulk microphysics scheme. Part I: Description and sensitivity analysis," *Mon. Wea. Rev.*, vol. 132, pp. 519-542, 2004.

[12] G. Thompson, P Field, R. Rasmussen, and W.l Hal, "Explicit forecasts of winter precipitation using an improved bulk microphysics scheme. Part II: Implementation of a new snow parameterization," *Mon. Wea. Rev.*, vol. 136, pp. 5095-5115, 2008.

[13] Z. I. Janjic, "Nonsingular implementation of the Mellor–Yamada level 2.5 scheme in the NCEP Meso model," in *NCEP Office Note 437*, 2002, p. 61.

[14] ISO 12494, "Atmospheric icing of structures," Geneva, Switzerland, ISO 12494, 2001.

[15] L. Makkonen, "Models for the growth of rime, glaze, icicles and wet snow on structures," *Phil. Trans. R. Soc. London*, vol. 358, pp. 2913-2939, 2000.

[16] K. J. Finstad, E. P. Lozowski, and E. M. Gates, "A computational investigation of water droplet trajectories," *J. Atmos. Oceanic Technol.*, vol. 5, no. 1, pp. 160-170, 1988.

[17] S. P. Ísaksson, Á. J. Elíasson, and E. Thorsteins, "Icing Database—Acquisition and registration of data," in *Proc. Eighth Int. Workshop on Atmospheric Icing of Structures (IWAIS)*, Reykjavik, 1998, pp. 235-240.

[18] Ó. Rögnvaldsson, H. Ágústsson, and H. Ólafsson. (2009) Stöðuskýrsla vegna þriðja árs RÁVandar verkefnisins. [Online]. ftp://ftp.betravedur.is/pub/publications/RAV-stoduskyrsla2009.pdf

[19] F. H. Sigurðsson, "Ísingarhætta og háspennulína yfir hálendið," *Veðrið*, vol. 16, no. 2, pp. 53-58, 1971.

[20] Á. J. Eliasson and E. Thorsteins, "Ice load measurements in test spans for 30 years," in *12th IWAIS*, Yokohama, Japan, October 2007.